

**Nature and Hydrocarbon Potential of Organic Matter in Offshore Mahanadi Basin,  
East Coast of India**

**Subhashree Mishra<sup>a</sup>, Aditya Peketi<sup>a</sup>, Bodhisatwa Hazra<sup>b</sup>, Rheane Da Silva<sup>a,c</sup>, Aninda  
Mazumdar<sup>a\*</sup>**

<sup>a</sup>CSIR-National Institute of Oceanography, Goa, India-403004

<sup>b</sup>CSIR-Central Institute of Mining and Fuel Research, Dhanbad, India-826001

<sup>c</sup>St. Xavier's college, Goa, India-403507

\*E-mail address: maninda@nio.org

**Abstract**

Evaluating the hydrocarbon generating potential of buried organic matter in marine sediments is critical in offshore petroleum exploration. Organic matter sources, total organic matter content, and maturity state play key roles in hydrocarbon generation when subjected to suitable temperature-pressure conditions. In the present study, we have characterized organic matter source and maturity to evaluate the hydrocarbon generating potential of organic matter in the offshore Mahanadi Basin along the east coast of India. Although onshore hydrocarbon reservoirs, including coal, coalbed methane (CBM) & shale gas, are extensively explored in the Mahanadi Basin, a systematic characterization of the offshore buried organic matter is lacking. Towards this endeavour, we have adopted an integrated approach using TOC, (TOC/TN)<sub>m</sub>, Rock-Eval pyrolysis, and bulk carbon isotopic analyses. Organic geochemical screening (Rock-Eval pyrolysis) reveals predominance of Type III and IV kerogen, with TOC content ranging from 0.61-1.71 wt.%. The Hydrogen Index (HI) values (23-168 mg HC/g TOC) infer that the organic matter is prone to generate gaseous hydrocarbons. Bi-modal distribution pattern of the S2 peak observed in six samples suggests the presence of both labile and refractory organic matter. The (TOC/TN)<sub>m</sub> ratios and  $\delta^{13}\text{C}_{\text{TOC}}$  values indicate that the organic matter is derived from both terrestrial and marine sources.

**Keywords**

Hydrocarbon potential; Organic matter source; Marine Sediments; Total organic carbon; Pyrolysis

## 1. Introduction

Hydrocarbon generation potential of marine organic matter (Hare et al., 2014; Ratnayake et al., 2018; Baiyegunhi et al., 2020) is linked to the source and nature of organic matter, total organic carbon (TOC) content, and thermal maturity (Conford, 1998; Carvajal-Ortiz and Gentzis, 2015; Gordon et al., 2021). The marine sedimentary organic matter is derived from multiple sources ranging from terrestrial to marine (Liu et al., 2015). The allochthonous organic matter is delivered through riverine flow, aeolian transportation and autochthonous organic matter represents marine primary and regenerated productions (Maksymowska et al., 2000; Szymczak-Zyła and Lubecki, 2022). The autochthonous labile organic matter is primarily responsible for the generation of oil and condensate (Tissot and Welte, 1984); whereas, the allochthonous organic matter is considered a major source of the generation of gas (Combaz and De Matharel, 1978; Snowdon and Powell, 1982; Kang et al., 2020). A TOC content of >0.5 wt. % in sediments is a good source for hydrocarbon generation (Peters, 1986; Nuñez-betelu and Baceta, 1994; Carvajal-Ortiz and Gentzis, 2015). Rock-Eval pyrolysis and stable carbon isotopic ( $\delta^{13}\text{C}_{\text{TOC}}$ ) values of TOC have been extensively used to investigate the sources, nature and hydrocarbon generation potential of organic matter in marine sediments (Holtvoeth et al., 2001; Galimov, 2004; Carrie et al. 2012; Ramachandran et al., 2013; Hare et al., 2014; Baudin et al., 2015; Liu et al., 2015; Ratnayake et al., 2018; Asaoka et al., 2020; Gordon et al., 2021; Szymczak-Zyła and Lubecki, 2022).

Hydrocarbon potential and maturity of sedimentary organic matter from Mannar (Ratnayake et al., 2018) and Krishna-Godavari (K-G) offshore (Ramachandran et al., 2013), east coast India show the presence of type II-III and type III kerogen respectively. The Mahanadi basin is currently emerging as a hub for hydrocarbon exploration and production activities (Datta et al., 2012; Guru Rajesh et al., 2019).

In the present study, a 39 m long sediment core (~300 ky) from Mahanadi offshore region (water depth: 1480 m) has been analysed for organic matter sources and hydrocarbon generating potential. A total of twenty-five sediment samples were evaluated using various parameters such as total organic carbon (TOC), Rock-Eval pyrolysis, (total organic carbon/total nitrogen)<sub>molar</sub> [(TOC/TN)<sub>m</sub>], and carbon isotope ratio measurement. The pyrolysis technique is widely used to identify the type of organic matter, assess the potentiality for oil/gas generation, and thermal maturity (Tissot and Welte 1978; Peters 1986; Varma et al., 2015; Baudin et al., 2015; Mishra et al., 2016; Wood and Hazra 2017, 2018; Hazra et al., 2019, 2021).

## 2. Geology

The Mahanadi Basin (Fig. 1) is a significant sedimentary basin with respect to offshore hydrocarbon potential (Singh, 2008). The pull-apart basin formed due to rifting of the Gondwana Land during Jurassic-Early Cretaceous period (Jagannathan et al., 1983; Fuloria et al., 1992). It ranges in the north from Jagannathpur to Chilka lake in the south and discharge the carrying sediment load eastwardly to the offshore in the Bay of Bengal as shown in the geological map Fig. 1 (Mazumdar et al., 2015). The basin covers an area of ~ 2,60,000 km<sup>2</sup> and reaches a water depth of more than 3000 m with deeper offshore area significantly greater than the shallow offshore (Singh, 2008; Mazumdar et al., 2014, 2015; DGH petroleum basin report, 2022). Stratigraphically, Mahanadi offshore sedimentary succession may be divided into Cretaceous, Paleogene, and Neogene deposits. The Lower Cretaceous intertrappeans and volcanic are successively overlain by Paleocene sand/silt/clay, Eocene carbonate, Lower to Middle Miocene clay/silt/minor limestone, and Pliocene to Younger sand/silt/clay (Jagannathan et al., 1983; Kaila et al., 1987; Fuloria et al., 1992; Singh, 2008). The top 40 m of the core studies in the present work are composed of loose sands, clays, and silts conformably overlying to Neogene sediments (Mazumdar et al. 2015).

The Mahanadi River system including the tributaries (Seonath, Mand, Jonk, Hasdeo, Ib, Ong and Tel) discharges the sediment load into the offshore areas. The average clay mineral contents in the Mahanadi basin sediment are illite: 24.6 to 54.4 (average: 38% ± 7.4); smectite: 19.7 to 59.4 (average: 35% ± 9.3); and chlorite + kaolinite: 15.1 to 35.1 (average: 27% ± 6.6) (Mazumdar et al., 2015; Peketi et al 2021). The reported TOC contents in Mahanadi offshore sediments range from 0.15 to 3 wt % (Da Silva et al., 2017, DGH petroleum basin report, 2022). The Mahanadi river drains and erodes the coal-bearing horizons on land which is incorporated in the detrital load.

## 3. Methodology

Twenty-five samples were selected from a 39 m piston core collected during ORV Marion Dufresne (MD161, station 19). The core was collected from a water depth of 1480 m (Lat. 18°59.1020'N; Long. 85°41.1669' E) using a calypso piston corer (Da Silva et al., 2017). The sediment samples were freeze-dried, desalinated, decarbonated and homogenized (finely ground) using an agate mortar – pestle prior to Rock-Eval pyrolysis analysis. Total carbon and total nitrogen contents were determined with an elemental analyser (Thermo EA1112) using desalinated samples. Total inorganic carbon content was determined using an UIC coulometer (CM 5330). 2,4-DNP was used to prepare the calibration standard for TOC and TN measurements. MAG-I standard was used to check the reproducibility of the carbon and nitrogen contents analysis. Reproducibility of TC and TN was found to be better than 0.2 and 0.03

% respectively. Total organic carbon content was determined by subtracting the inorganic carbon content from the total carbon content. High pure CaCO<sub>3</sub> (sigma-Aldrich) was used as standard for TIC determination and the measured values were within 12 ± 0.25 %. The carbon isotope ( $\delta^{13}\text{C}_{\text{TOC}}$ ) ratios were measured using decarbonated sediment samples with stable isotope ratio mass spectrometer (Thermo Delta-V-plus) coupled with an elemental analyzer (Thermo EA 1112). The lab tank (CO<sub>2</sub>) was calibrated using cellulose standard (IAEA-C3;  $\delta^{13}\text{C}$ : - 24.7 ± 0.1 ‰ (VPDB)). The external precision calculated for  $\delta^{13}\text{C}$  is typically 0.07-0.09 ‰. The results of TOC, (TOC/TN)<sub>m</sub> and carbon isotope ( $\delta^{13}\text{C}_{\text{TOC}}$ ) values were adopted from Da Silva et al. (2017).

The Rock-Eval pyrolysis analysis was carried out using Rock-Eval 6 (Vinci Technologies) equipment at CSIR-CIMFR Dhanbad, India. The sediment samples were analysed using the built-in bulk rock/basic cycle method following Lafargue et al. (1998) and Behar et al. (2001). Approximately 10-20 mg of desalinated homogenized sediment samples are introduced into the pyrolysis oven in presence of nitrogen (inert) atmosphere and heated at 300 °C for 3 minutes. At this stage, adsorbed short-chain lipids and other volatile fractions are released and recorded as S1 peak. This stage is followed by a temperature ramping of 25 °C/min till up to 650 °C. During this phase, the heavier hydrocarbons are liberated due to the thermal cracking of larger molecules and recorded as S2 peak. The hydrocarbons liberated as S1 and S2 peak are detected and quantified using a flame ionization detector (FID). The temperature (°C) at which maximum amount of hydrocarbons (S2) are generated from the samples is designated as T<sub>max</sub> which is routinely assumed to be an indicator of the thermal maturity of the kerogen (Hunt, 1996; Hazra et al., 2019). During this pyrolysis program, carbon dioxide (CO<sub>2</sub>) and carbon monoxide (CO) released along with the hydrocarbons are continuously measured by infrared (IR) spectroscopy documented as S3 peak (Lafargue et al., 1998; Hazra et al., 2021). Other parameters like hydrogen index (HI), oxygen index (OI), production index (PI) and potential yield (PY) were calculated using the pyrolysis data following Peters, (1986). HI ( $\frac{S2}{\text{TOC}} \times 100$ ) denotes the quantity of hydrogen present in pyrolysable organic compounds (S2 peak) relative to the TOC content in the sample (mg HC/g TOC). OI ( $\frac{S3}{\text{TOC}} \times 100$ ) corresponds to the quantity of CO/CO<sub>2</sub> (S3 peak) relative to the TOC content in the studied sediments and denoted as mg CO<sub>2</sub>/g TOC). PI ( $\frac{S1}{(S1+S2)}$ ) is the ratio of free hydrocarbons to total amount of hydrocarbons generated from the samples and denoted as mg HC/g. PY (S1 + S2) also known as genetic potential of the sample and is assessed by adding the amount of free hydrocarbons and heavier hydrocarbons (mg HC/g) (Peters, 1986; Mishra et al., 2016).

## 4. Results

Total organic carbon content,  $(\text{TOC}/\text{TN})_m$ ,  $\delta^{13}\text{C}_{\text{TOC}}$  and Rock-Eval pyrolysis data are presented in Table 1. The TOC content and  $(\text{TOC}/\text{TN})_m$  ratios ranges from 0.61 to 1.71 wt.% and 9.2 to 16.2 respectively. Representative Rock-Eval pyrograms are presented in figure 2 showing unimodal (Fig. 2a) and bi-modal (Fig. 2b) S2 peaks respectively. The  $T_{\text{max}}$  shows a large variation from 328 to 612 °C (Table 1). The S1 values range from 0.07-0.19 mg HC/g. The S2 and S3 values range from 0.33 to 1.46 mg HC/g and 1.79 to 5.43 mg  $\text{CO}_2/\text{g}$  respectively. The kerogen type is plotted in the HI vs  $T_{\text{max}}$  cross plots (Fig. 3) and HI vs OI (Fig. 4). The HI and OI values range from 23 to 156 mg HC/g TOC and 195 to 548 mg  $\text{CO}_2/\text{g}$  TOC respectively (Fig. 4). The hydrocarbon generating potential of the organic matter is represented in the TOC vs S2 cross plot (Fig. 5). The  $\delta^{13}\text{C}_{\text{TOC}}$  values of sediment samples ranging between -21.1 to -16.7‰ (Fig. 6).

## 5. Discussions

The nature and amount of organic matter in marine sediments are important parameters to evaluate the source and hydrocarbon generative potential (Barker, 1979; Baiyegunhi et al., 2020). The TOC content (0.61–1.71 wt.%; avg.:  $0.97 \pm 0.25$ ) of the studied samples (Table-1) indicates the presence of adequate amount of organic matter required to generate liquid (oil) or gaseous hydrocarbons (Tissot and Welte, 1984; Baiyegunhi et al., 2020). Two contrasting pyrograms (Fig. 2) were observed in the present study. The pyrograms of nineteen samples are showing cracking of organic matter at low pyrolysis temperature ( $T_{\text{max}}$ : 328-414 °C) due to predominance of immature organic matter (Representative pyrogram, Fig. 2a), whereas six sediment samples display two distinct S2 peaks (Fig. 2b) denoting presence of two kinds of organic matter (low maturity organic matter,  $T_{\text{max}} < 400$  °C and high maturity organic matter,  $T_{\text{max}} > 600$  °C) (Holtvoeth et al., 2001, 2003). Holtvoeth et al. (2001) have also reported the presence of three types of organic matter such as labile marine organic components, low mature terrigenous source and high mature land-derived inert/ oxidised fractions. Bimodal distribution of S2 peak has also been reported by Hare et al. (2014) and Baudin et al. (2015) in marine sediments. The  $T_{\text{max}}$  values  $< 435$  °C denotes an immature state of the organic matter, whereas,  $T_{\text{max}}$  ranging from 435 - 450 °C suggests an early to peak stage of maturity. The  $T_{\text{max}}$  values ranging from 450-470 °C and more than 470 °C represent late mature (good for oil generation) and post mature (appropriate for generation of gas) organic matter respectively (Tissot et al., 1974; Tissot and Welte, 1984; Peters, 1986; Hunt, 1996; Kang et al., 2020; Yang and Horsfield, 2020). The binary plot of  $T_{\text{max}}$  vs. HI (Fig. 3) also elucidates that majority of the samples (nineteen) fall within the immature zone and only six samples are the post mature zone (Peters and Simoneit, 1982; Langford

and Blanc-Valleron, 1990). These six samples possibly represent over-matured or highly refractory (oxidized) organic matter (Holtvoeth et al., 2001).

The data cluster on the Van Krevelen diagram (HI and OI cross plot: Fig. 4) fall within the kerogen type III and type IV mixed zone suggesting primarily gas prone nature of the organic matter in Mahanadi basin sediments. Initial hydrocarbon exploration in deeper shelf area of Mahanadi basin has revealed the presence of biogenic and biogenic-thermogenic mixed hydrocarbon gases (Datta et al., 2012). The gas composition reported by Datta et al. (2012) suggests a mixture of dry (primarily methane) and wet gas which corroborates our findings. The type III kerogens are mainly derived from terrestrial plant source having potential for wet gas generation, while type IV is relict of extreme alteration/in-situ oxidation of organic matter with potential for dry gas generation (Tissot et al., 1974; Tissot and Welte, 1984; Peters, 1986; Ibrahimbas and Riediger, 2004; Dembicki, 2009; Mendhe et al., 2018; Baiyegunhi et al., 2020). Our data further suggests poor petroleum generation potential of the Mahanadi Basin sediment organic matter (Fig. 5).

The type of kerogen and the hydrocarbon generation potential (Gordon et al., 2021; Szymczak-Zyła and Lubecki, 2022) depends on relative contribution of various organic matter sources (Holtvoeth et al., 2001; Ramachandran et al., 2013). The  $(\text{TOC}/\text{TN})_m$  ratio vs  $\delta^{13}\text{C}_{\text{TOC}}$  plot (Fig. 6; Tyson, 2012; Volvoikar et al., 2020) of MD/161-19 suggests mixed terrestrial and marine organic input. The data cluster has marine organic source as one of the end members, however, absence of a well-defined mixing line (trend line) indicates variable contribution of both C3 and C4 vegetation as terrestrial input. Based on organic geochemistry and compound specific C-isotope ratio measurement Da Silva (2018) has also suggested mixed a marine C3-C4 sources for the Mahanadi Basin sediments (Da Silva et al., 2017). The terrestrial organic matter is subjected to extensive oxidative degradation during transportation leading to loss of most labile components responsible for petroleum generation. In other words, the residual kerogen (type III-IV) of Mahanadi basin sediment is more amenable to gas generation rather oil generation. The pyrolysis data further suggest presence of highly refractory organic matter fraction in some of the samples resulting in bi-modal pattern of S2 peak. This high  $T_{\text{max}}$  component is present throughout the core and may be attributed to lithogenic recycled organic matter which possibly represents the high maturity (HM) component. The latter component needs further investigation and characterization.

## 6. Summary and Conclusions

A combination of Rock-Eval pyrolysis, stable carbon isotope analysis and carbon-nitrogen elemental ratios of Mahanadi Basin sediment samples suggest presence of kerogen type-III and IV

which are prone to hydrocarbon gas generation. The  $(\text{TOC}/\text{TN})_m$  ratios and  $\delta^{13}\text{C}_{\text{TOC}}$  values imply a mixed marine-C3-C4 sources for the sediment kerogen. The bimodal distribution of the  $T_{\text{max}}$  (S2 peak) indicates the presence of low mature (LM) and high mature (HM) kerogen fractions. The present study certainly helps to evaluate the hydrocarbon generation potential of the organic matter from the offshore Mahanadi sediments which may be a guide for oil/gas exploration in future.

### **Conflict of Interests**

The authors declare that they have no known competing financial interests or personal relationships that could have appeared to influence the work reported in this paper.

### **Author contributions**

**Subhashree Mishra:** Conceptualisation, Investigation, Writing-original draft. **Aditya Peketi:** Investigation, editing the manuscript. **Bodhisatwa Hazra:** Analytical part, Methodology. **Rheane Da Silva:** Sample collection, methodology. **Aninda Mazumdar:** Conceptualisation, investigation, Writing.

### **Acknowledgements**

We acknowledge the Director, CSIR–NIO for supporting this study, the MOES (GAP2303) and MLP 2015 for providing funds for the acquisition of sediment cores and data. Sincere thanks to the Director, CSIR-CIMFR for extending the analytical support.

### **References**

- Asaoka, S., Jadoon, W.A., Umehara, A., Takeda, K., Otani, S., Ohno, M., Fujitake, N., Sakugawa, H., Okamura, H., 2020. Organic matter degradation characteristics of coastal marine sediments collected from the Seto Inland Sea, Japan. *Mar. Chem.* 225, 103854.
- Baiyegunhi, T.L., Liu, K., Gwavava, O., Wagner, N., Baiyegunhi, C., 2020. Geochemical Evaluation of the Cretaceous Mudrocks and Sandstones (Wackes) in the Southern Bredasdorp Basin, Offshore South Africa: Implications for Hydrocarbon Potential. *Minerals* 10(7), 595.
- Barker, C., 1979. Organic geochemistry in petroleum exploration. AAPG (Education Course Note Series) 10, 159.
- Baudin, F., Disnar, J.R., Aboussou, A., Savignac, F., 2015. Guidelines for Rock-Eval analysis of recent marine sediments. *Org. Geochem.* 86, 71-80.
- Behar, F., Beaumont, V., Penteado, H.L., De, B., 2001. Rock-Eval 6 Technology: Performances and Developments. *Oil & Gas Science and Technology – Rev IFP* 56(2), 111-134.
- Carrie, J., Sanei, H., Stern, G., 2012. Standardisation of Rock-Eval pyrolysis for the analysis of recent sediments and soils. *Org. Geochem.* 46, 38-53.

- Carvajal-Ortiz, H., Gentzis, T., 2015. Critical considerations when assessing hydrocarbon plays using Rock-Eval pyrolysis and organic petrology data: data quality revisited. *Int. J. of Coal Geol.* 152, 113–122.
- Combaz, A., De Matharel, M., 1978. Organic sedimentation and genesis of petroleum in Mahakam delta, Borneo. *AAPG Bulletin* 62, 1684.
- Conford, C., 1998. Source rocks and hydrocarbons of The North Sea. In: Glennie, K.W. (Ed.), *Petroleum Geology of the North Sea*. Blackwell, Oxford, 376–462.
- Da Silva, R., Mazumdar, A., Mapder, T., Peketi, A., Joshi, R.K., Shaji, A., Mahalakshmi, P., Sawant, B., Naik, B.G., Carvalho, M.A., Molletti, S.K., 2017. Salinity stratification-controlled productivity variation over 300ky in the Bay of Bengal. *Sci. Rep.* 7, 14439.
- Da Silva, R., 2018. Elucidation of paleoclimatic fluctuations from organic and inorganic proxies: A case study from the Mahanadi basin, Bay of Bengal, Published PhD Thesis, Department of Marine Science, Goa University. <http://hdl.handle.net/10603/286752>.
- Datta, S., Mukhopadhyay, P., Das, D., Das, P.K., 2012. Hydrocarbon Occurrences in Mahanadi Basin. 9<sup>th</sup> Biennial International Conference and Exposition on Petroleum Geophysics, SPG India.
- Dembicki, H., 2009. Three common source rock evaluation errors made by geologists during prospect or play appraisals. *AAPG Bulletin* 93, 341–356.
- DGH petroleum basin report, 2022. Basin Introduction: Mahanadi – NEC Basin.
- Fuloria, R.C., Pandey, R.N., Bharali, B.R., Mishra, J.K., 1992. Stratigraphy, Structure and Tectonics of Mahanadi Offshore Basin. Geological Survey of India (Special Publication) No. 9, 255-265.
- Galimov, E.M., 2004. The pattern of  $d^{13}C_{org}$  versus HI/OI relation in recent sediments as an indicator of geochemical regime in marine basins: comparison of the Black Sea, Kara Sea, and Cariaco Trench. *Chem. Geol.* 204, 287– 301.
- Gordon, J.B., Sanei, H., Ardakani, O., Pedersen, P.K., 2021. Effect of sediment source on source rock hydrocarbon potential; An example from the Kimmeridgian and Tithonian-aged source rocks of the central ridge, offshore Newfoundland, Canada. *Mar. Petrol. Geol.* 127, 104965.
- Guru Rajesh, K., Mahapatra, C., Mishra, B.M., Pradhan, B.N., Das, S.K., 2019. Surface gas seepages in the on-land Mahanadi Basin: implications for shallow biogenic gas prospectivity. *ONGC Bulletin* 54 (1), 55-72.
- Hare, A.A., Kuzyk, Z.Z.A., Macdonald, R.W., Sanei, H., Barber, D., Stern, G.A., Wang, F., 2014. Characterization of sedimentary organic matter in recent marine sediments from Hudson Bay, Canada, by Rock-Eval pyrolysis. *Org. Geochem.* 68, 52–60.
- Hazra, B., Singh, D.P., Crosdale, P.J., Singh, V., Singh, P.K., Gangopadhyay, M., Chakraborty, P., 2021. Critical insights from Rock-Eval analysis of vitrains. *Int. J. of Coal Geol.* 238, 103717.
- Hazra, B., Karacan, C.Ö., Tiwari, D.M., Singh, P.K., Singh, A.K., 2019. Insights from Rock-Eval analysis on the influence of sample weight on hydrocarbon generation from lower Permian organic matter rich rocks, West Bokaro basin, India. *Mar. Pet. Geol.* 106, 160–170.



- Holtvoeth, J., Wagner, T., Horsfield, B., Schubert, C.J., Wand, U., 2001. Late-Quaternary supply of terrigenous organic matter to the Congo deep-sea fan (ODP site 1075): implications for equatorial African paleoclimate. *Geo. Mar. Lett.* 21, 23-33.
- Holtvoeth, J., Wagner, T., Schubert, C., 2003. Organic matter in river-influenced continental margin sediments: The land-ocean and climate linkage at the Late Quaternary Congo fan (ODP Site 1075). *G-cubed* 4(12), 1109.
- Hunt, J.M., 1996. *Petroleum Geochemistry and Geology*. WH Freeman and Company, New York, 332 p.
- Ibrahimbas, A., Riediger, C., 2004. Hydrocarbon source rock potential as determined by Rock-Eval 6/TOC pyrolysis, Northeast British Columbia and Northwest Alberta. British Columbia Ministry of Energy, Mines and Petroleum Resources, Summary of Activities 7-18.
- Jagannathan, C.R., Ratnam, C., Baishya, N.C., Das Gupta, U., 1983. Geology of the offshore Mahanadi Basin. *Petrol. Asia J.* 6, 101-104.
- Kaila, K.L., Tewari, H.C., Mall, D.M., 1987. Crustal structure and delineation of Gondwana Basin in Mahanadi Delta Areas, India from deep seismic sounding. *J. of Geol. Soc. of India* 3, 293-308.
- Kang, S., Shao, L., Qin, L., Li, S., Liu, J., Shen, W., Chen, X., Eriksson, K.A., Zhou, Q., 2020. Hydrocarbon Generation Potential and Depositional Setting of Eocene Oil-Prone Coaly Source Rocks in the Xihu Sag, East China Sea Shelf Basin. *ACS Omega* 5, 32267–32285.
- Lafargue, E., Marquis, F., Pillot, D., 1998. Rock-Eval 6 applications in hydrocarbon exploration, production, and soil contamination studies. *Revue de l'institut français du pétrole* 53(4), 421-437.
- Langford, F.F., Blanc-Valleron, M.M., 1990. Interpreting Rock–Eval pyrolysis data using graphs of pyrolyzable hydrocarbons vs. total organic carbon. *AAPG Bulletin* 74, 799-804.
- Liu, D., Li, X., Emeis, K-C., Wang, Y., Richard, P., 2015. Distribution and sources of organic matter in surface sediments of Bohai Sea near the Yellow River Estuary, China. *Estuar. Coast. Shelf Sci.* 165, 128-136.
- Maksymowska, D., Richard, P., Piekarek-Jankowska, H., Riera, P., 2000. Chemical and Isotopic Composition of the Organic Matter Sources in the Gulf of Gdansk (Southern Baltic Sea). *Estuar. Coast. Shelf Sci.* 51, 585–598.
- Mazumdar, A., Kocherla, M., Carvalho, M.A., Peketi, A., Joshi, R.K., Mahalaxmi. P., Joao, H.M., Jisha, R., 2015. Geochemical characterization of the Krishna-Godavari and Mahanadi offshore basin (Bay of Bengal) sediments: A comparative study of provenance. *Mar. Petrol. Geol.* 60, 18-33.
- Mazumdar, A., Peketi, A., Joao, H.M., Dewangan, P., Ramprasad, T., 2014. Pore-water chemistry of sediment cores off Mahanadi Basin, Bay of Bengal: possible link to deep seated methane hydrate deposit. *Mar. Petrol. Geol.* 49, 162-175.
- Mendhe, V.A., Mishra, S., Varma, A.K., Kamble, A.D., Banerjee, M., Singh, B.D., Sutay, T.M., Singh, V.P., 2018. Geochemical and petrophysical characteristics of Permian shale gas reservoirs of Raniganj Basin, West Bengal, India. *Int. J. of Coal Geol.* 188, 1-24.

- Mishra, S., Mendhe, V.A., Kamble, A.D., Bannerjee, M., Varma, A.K., Singh, B.D., Pandey, J.K., 2016. Prospects of shale gas exploitation in Lower Gondwana of Raniganj Coalfield (West Bengal), India. *The Palaeobotanist* 65, 31–46.
- Nuñez-betelu, L., Baceta, J.I., 1994. Basics and application of rock-eval/TOC pyrolysis: an example from the uppermost paleocene/lowermost Eocene in the Basque Basin, Western Pyrenees. *San Sebastian* 46, 43-62.
- Peketi, A., Mazumdar, A., Pillutla, S. P. K., Sawant, B., Gupta, H., 2021. Climatic and Tectonic Control on the Bengal Fan Sedimentation Since the Pliocene. *G-cubed* 22, e2020GC009448. <https://doi.org/10.1029/2020GC009448>.
- Peters, K.E., 1986. Guidelines for Evaluating Petroleum Source Rock Using Programmed Pyrolysis. *AAPG Bulletin* 70, 318-329.
- Peters, K.E., Simoneit, B.R.T., 1982. Rock-Eval Pyrolysis of Quaternary Sediments from Leg 64, Sites 479 and 480, Gulf of California.
- Ramachandran, K., Babu, V., Behera, B.K., Harinarayana, T., 2013. Source rock analysis, thermal maturation and hydrocarbon generation using Rock-Eval pyrolysis in parts of Krishna–Godavari basin, India: a case study. *J. Pet. Explor. Prod. Technol.* 3, 11–20.
- Ratnayake, A.S., Kularathne, C.W., Sampei, Y., 2018. Assessment of hydrocarbon generation potential and thermal maturity of the offshore Mannar Basin, Sri Lanka. *J. Pet. Explor. Prod. Technol.* 8, 641–654.
- Singh, L., 2008. Mahanadi Basin (Mahanadi-NEC Basin) Oil and Gas Fields of India. *Indian Petroleum Publishers, Dehradun, India* 325-346.
- Snowdon, L., Powell, T., 1982. Immature oil and condensate. A modification to the hydrocarbon generation model for terrestrial organic matter. *AAPG Bulletin* 66(6), 775-788.
- Szymczak-Zyła, M., Lubecki, L., 2022. Biogenic and anthropogenic sources of sedimentary organic matter in marine coastal areas: A multi-proxy approach based on bulk and molecular markers. *Mar. Chem.* 239, 104069.
- Tissot, B., Welte, D.H., 1978. *Petroleum Formation and Occurrence*. Springer-Verlag, Berlin 538 p.
- Tissot, B., Durand, B., Espitalie, J., Combaz, A., 1974. Influence of nature and diagenesis of organic matter in formation of petroleum. *AAPG Bulletin* 58(3), 499-506.
- Tissot, B.P., Welte, D.H., 1984. *Petroleum Formation and Occurrence*. 2<sup>nd</sup> Edition, Springer-Verlag, Berlin, 699p.
- Tyson, R.V., 2012. *Sedimentary organic matter: Organic facies and palynofacies*. Springer Science and Business Media, B.V.
- Varma, A.K., Hazra, B., Mendhe, V.A., Chinara, I., Dayal, A.M., 2015. Assessment of organic richness and hydrocarbon generation potential of Raniganj basin shales, West Bengal, India. *Mar. Petrol. Geol.* 59, 480-490.

- Wood, D.A., Hazra, B., 2017. Characterisation of organic-rich shales for petroleum exploration & exploitation: A review-part 2: Geochemistry, thermal maturity, isotopes and biomarkers. *J. Earth Sci.* 28(5), 758-778.
- Wood, D.A., Hazra, B., 2018. Pyrolysis S<sub>2</sub>-peak characteristics of Raniganj shales (India) reflect complex combinations of kerogen kinetics and other processes related to different levels of thermal maturity. *Adv. Geo-Energy Res.* 2(4), 343-368.
- Yang, S., Horsfield, B., 2020. Critical review of the uncertainty of T<sub>max</sub> in revealing the thermal maturity of organic matter in sedimentary rocks. *Int. J. of Coal Geol.* 225, 103500.
- Volvoikar, S., Mazumdar, A., Peketi, A., Dewangan, P., Sawant, B., Manaskanya, A., Goswami, H., Das, D., Pujari, S., 2020. Contrasting sulfidization in the turbidite and hemipelagic sediments of Bengal Fan. *Marine and Petroleum Geology* 118, 104408.

### Figure and Table captions:

Fig. 1: Map of the study area showing the location of MD/161-19 core (red circle) in offshore Mahanadi Basin.

Fig. 2: Rock-Eval pyrograms for representative samples showing the unimodal and bi-modal distribution of the S2 peak.

Fig. 3: Plot of  $T_{max}$  versus Hydrogen Index showing nature and maturity of the organic matter.

Fig. 4: Plot of oxygen index versus hydrogen index showing kerogen types (Peters, 1986; Langford and Blanc Valleron, 1990).

Fig. 5: Plot of TOC and S2 representing potentiality of the organic matter in the offshore Mahanadi sediments.

Fig. 6: Relationship between  $(TOC/TN)_m$  and  $\delta^{13}C_{TOC}$  of organic matter in the offshore Mahanadi sediments. The direction of black dotted arrows indicate increasing contribution of C3, C4 organic matter on the bulk organic matter. Blue dotted line indicate  $(TOC/TN)_{molar}$  Redfield ratio. La- Lacustrine; Ma- Marine (Tyson 2012).

Table 1: Results of  $[(TOC/TN)_m]$ , TOC, Rock-Eval pyrolysis and carbon ( $\delta^{13}C_{TOC}$ ) isotope analysis.

Figures:

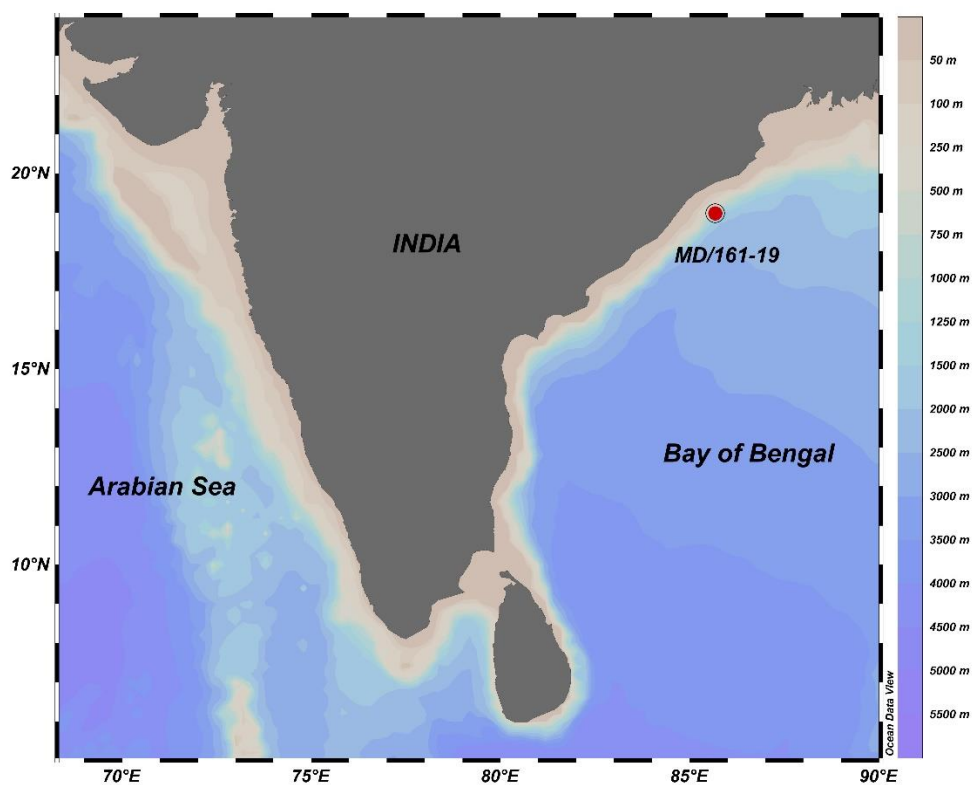


Fig. 1

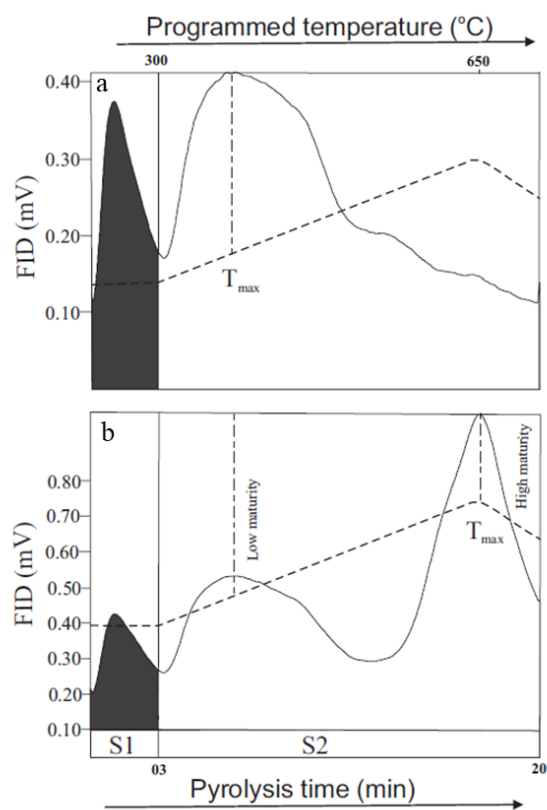


Fig. 2

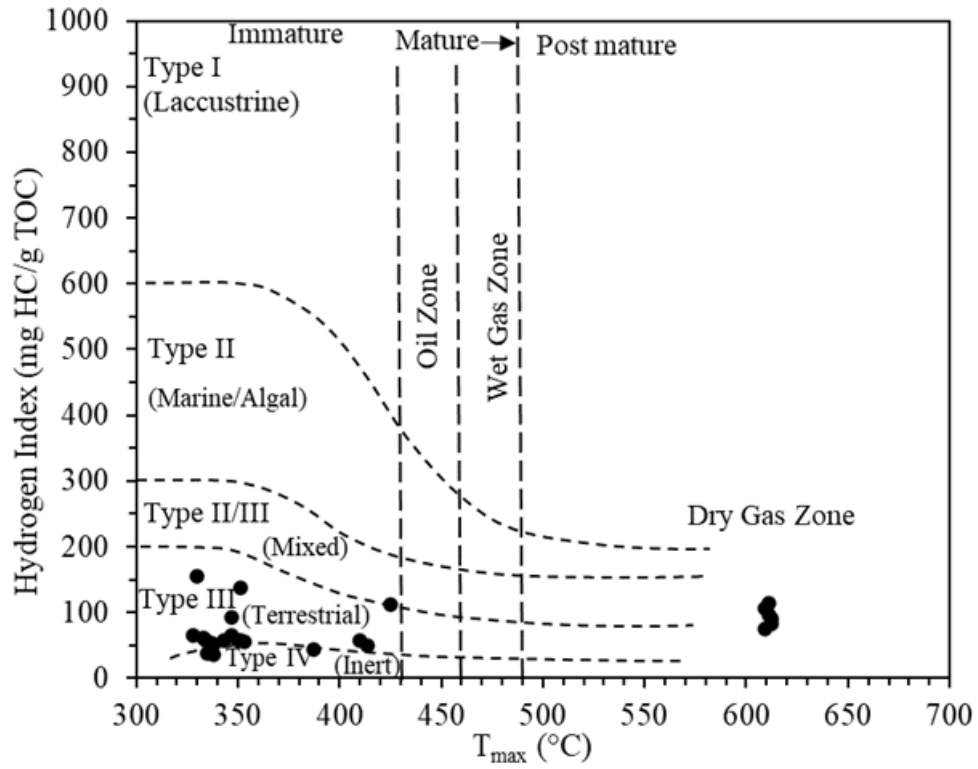


Fig. 3

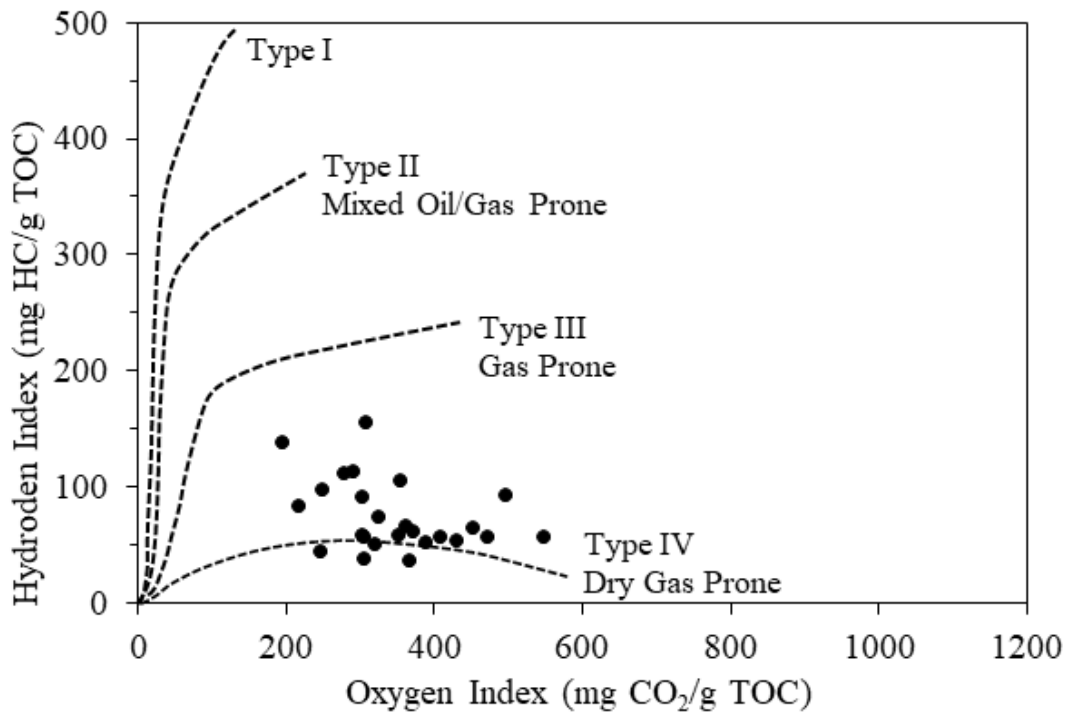


Fig. 4

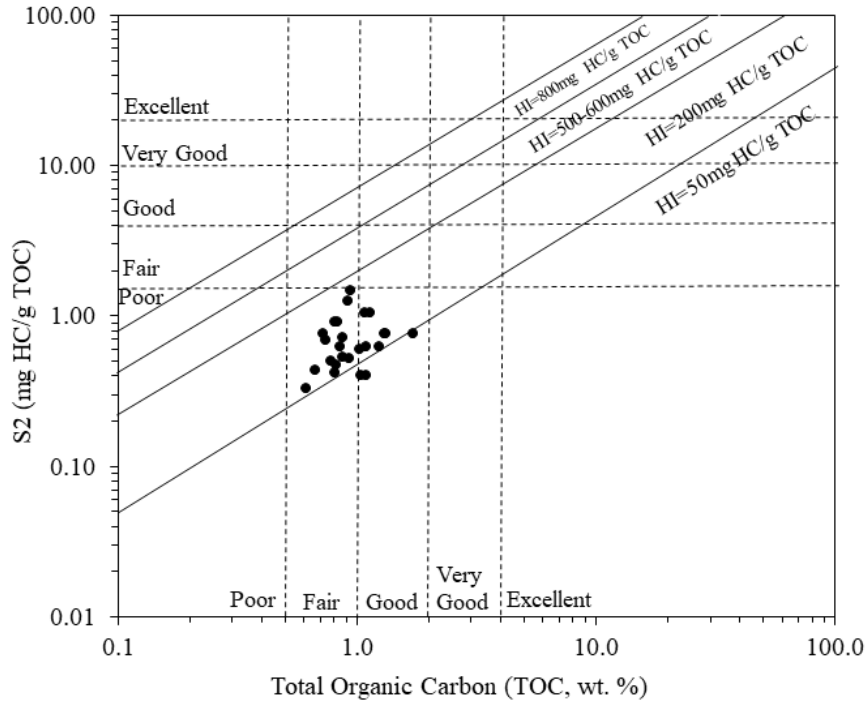


Fig. 5

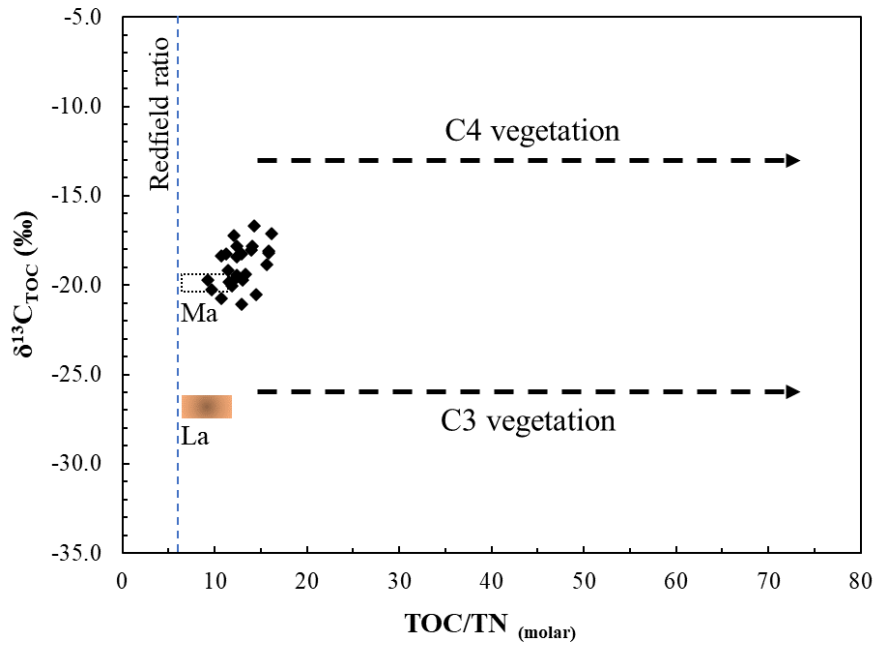


Fig. 6

Table 1:

Sl. No.	Age (KY)	Depth (cmbfsf)	(TOC/TN) <sub>m</sub>	TOC (wt. %)	S1 (mg HC/g)	S2 (mg HC/g)	S3 (mg CO <sub>2</sub> /g)	T <sub>max</sub> (°C)	HI (mg HC/g TOC)	OI (mg CO <sub>2</sub> /g TOC)	PI (mg HC/g)	PY (mg HC/g)	δ <sup>13</sup> C <sub>Toc</sub> (‰)
1	0.70	5	14.5	0.94	0.19	1.46	2.88	330	156	307	0.12	1.65	-20.5
2	15.05	463	12.4	1.31	0.16	0.76	4.61	350	58	353	0.17	0.92	-18.4
3	27.58	563	14.3	1.71	0.14	0.76	4.23	387	44	248	0.16	0.90	-16.7
4	71.35	923	10.7	0.77	0.10	0.50	3.51	347	65	453	0.17	0.60	-18.4
5	82.00	1188	16.2	1.09	0.10	0.62	3.34	334	57	305	0.14	0.72	-17.1
6	114.32	1803	12.9	0.81	0.08	0.92	2.36	611	114	292	0.08	1.00	-21.1
7	150.28	2328	12.4	0.93	0.10	0.52	5.09	353	56	548	0.16	0.62	-17.8
8	168.49	2433	11.2	0.67	0.08	0.44	2.44	328	65	363	0.15	0.52	-18.3
9	191.45	2543	11.5	0.92	0.14	1.26	1.79	351	137	195	0.10	1.40	-19.8
10	205.89	2678	12.9	0.85	0.08	0.63	2.77	609	74	326	0.11	0.71	-18.3
11	210.82	2773	11.8	0.87	0.07	0.72	1.91	612	83	219	0.09	0.79	-20.0
12	214.72	2848	13.0	1.07	0.09	1.04	2.69	611	97	250	0.08	1.13	-19.7
13	219.13	2933	12.1	0.82	0.08	0.47	3.88	351	57	473	0.15	0.55	-17.2
14	224.58	3038	9.2	0.61	0.07	0.33	2.64	337	54	430	0.18	0.40	-19.7
15	234.12	3128	12.3	0.72	0.09	0.76	2.56	609	106	356	0.11	0.85	-19.5
16	244.26	3223	9.7	0.74	0.13	0.69	3.69	347	93	498	0.16	0.82	-20.3
17	252.99	3298	14.1	1.24	0.10	0.62	3.97	414	50	320	0.14	0.72	-17.8
18	257.65	3338	15.6	1.32	0.14	0.76	5.43	410	57	410	0.16	0.90	-18.9
19	271.62	3458	13.9	0.81	0.08	0.42	3.16	338	52	390	0.16	0.50	-18.0
20	280.34	3533	13.4	1.14	0.12	1.04	3.46	612	91	304	0.10	1.16	-19.4
21	290.00	3623	15.8	1.09	0.08	0.40	4.00	338	37	367	0.17	0.48	-18.1
22	294.50	3668	15.8	1.04	0.07	0.40	3.17	335	39	305	0.15	0.47	-18.2
23	299.95	3733	11.5	0.87	0.09	0.53	3.23	333	61	372	0.15	0.62	-19.2
24	305.71	3803	12.1	1.03	0.12	0.60	3.13	343	58	304	0.17	0.72	-19.7
25	309.01	3843	10.8	0.83	0.14	0.92	2.30	425	111	279	0.13	1.06	-20.7

Abbreviation: KY: kiloyears; cmbfsf: cm below seafloor; TOC: total organic carbon content; TN: total nitrogen; HC: hydrocarbon; HI: hydrogen index; OI: oxygen index; PI: production index; PY: potential yield.